ISA Transactions 131 (2022) 299–310

Contents lists available at ScienceDirect

ISA Transactions

journal homepage: www.elsevier.com/locate/isatrans

Research article

On the existence of Equivalent-Input-Disturbance and multiple integral augmentation via H-Infinity Synthesis for unmatched systems

Burak Kürkçü [a,*], Coşku Kasnakoğlu [b], Mehmet Önder Efe [a], Rong Su [c]

[a] Department of Computer Engineering, Hacettepe University, Turkey
[b] Department of Electrical and Electronics Engineering, TOBB University of Economics and Technology, Turkey
[c] School of Electrical & Electronic Engineering, Nanyang Technological University, Singapore

ARTICLE INFO

Article history:
Received 8 June 2021
Received in revised form 23 April 2022
Accepted 24 April 2022
Available online 3 May 2022

Keywords:
Matched/Unmatched disturbances
MIMO disturbance observer
$\mathcal{H}_\infty$-Synthesis
Multiple integral augmentation
Hamiltonian matrices

ABSTRACT

In this paper, the existence of a solution for the transformation of the disturbances from the unmatched cases to the matched one is investigated. The usage of matched/unmatched disturbance notions and the underlying assumptions are clarified. Then, a simplified definition is introduced to obtain a set of performance metrics to be used in observer design. Using bilinear pole shifting and multiple integral augmentation to the plant, not only the stabilizability/detectability conditions but also infinity-norm bounds for unstable MIMO systems are derived. Then, the solvability of the augmented Hamiltonian matrices to get stabilizing solutions via standard $\mathcal{H}_\infty$-Synthesis is explained. Finally, the solutions, definitions, and assumptions are validated through numerical examples.

1. Introduction

Stability and performance are the prime issues in feedback control systems. A major factor, which deteriorates the closed-loop system's performance, is the presence of external disturbances. These external disturbances are classified as matched and unmatched(mismatched) disturbances based on whether they satisfy the matching condition or not. The mathematical formulation of the matching condition and its effects are defined in [1,2]. Numerous methods have been discussed the effects of the matching condition for disturbance compensation, including fault detection–estimation[3,4], a dual disturbance observer (DDO) based nonsingular terminal sliding mode control [5] and adaptive fault tolerant control under actuator failure and unmatched disturbances [6]. Moreover, as a significant challenge, it is stated that using disturbance observer-based techniques is restricted when the matching condition is not satisfied and requires some modification, including sum-of-squares method for synthesizing disturbance observer [7].

On the other hand, Equivalent-Input-Disturbance (EID) definition, which is introduced by [8,9], is one common and strong way to handle unmatched disturbances. This definition allows considering the exogenous disturbances in the equivalent form at the control input instead of rejecting them with a separate design that is dedicated to unmatched ones. This idea was experimentally validated in many control system design problems including, active disturbance rejection control [10], disturbance/uncertainty estimator based integral sliding mode control [11], and output feedback autopilot design for hypersonic vehicles [12]. Recently, researchers have been trying to improve EID-based control systems (so-called improved EID-IEID) to overcome the structural limitations of the conventional EID-based estimators [13]. To the best of our knowledge, although those EID and IEID methods work well under the given disturbances practically, all those works are leading us to [14] for guaranteeing the existence of the EID theoretically. However, [14], which uses non-casual stable inversion, is just valid under particular circumstances such as the system must be square (i.e., the same number of inputs and outputs), no zeros on the imaginary axis, and the output of the system should be polynomial, sinusoidal, or multiplication of these two.

Regardless of whether the disturbance is injected through the control channels or not, there are many assumptions on the disturbance or the system, which vary significantly. For instance, in [6], the derivative of the disturbance is assumed to be bounded by a known bound, [15] requires a square system, and [2,5] assumes that the disturbance is slowly time-varying, i.e., $\dot{d} \approx 0$. For the interested readers, further reading about the types of the disturbances can be found in [16]

Moreover, in the last decade, the necessity for a more general form of a disturbance model has received attention since some practical systems suffer from unbounded or fast-varying

* Correspondence to: Hacettepe University, Computer Engineering Building, room no: Z08, Beytepe Campus, 06800, Ankara, Turkey.
E-mail addresses: bkurkcu@cs.hacettepe.edu.tr (B. Kürkçü), kasnakoglu@etu.edu.tr (C. Kasnakoğlu), onderefe@gmail.com (M.Ö. Efe), rsu@ntu.edu.sg (R. Su).

https://doi.org/10.1016/j.isatra.2022.04.044
0019-0578/

disturbances/references [7,17]. In [18], a generalized disturbance observer for estimating polynomial-type disturbances in the time series expansion, is offered and it is stated that the general synthesis problem is still open. The work in [19] investigates the disturbance observer based control for uncertain nonlinear systems under polynomial-type disturbances and output measurement errors. The research in [20] considers the reference tracking problem under a polynomial-type reference signal.

With polynomial-ordered exogenous signals, the internal model principle (IMP) is one of the fundamental approaches for the reference tracking or the disturbance rejection. When the model of the exogenous signal is known, the IMP can stabilize the system and can achieve the zero-error goal [21]. The major limitation of the IMP is that it requires an accurate model of those signals a priori [22]. To solve this issue, some key and successful remedies were offered. In [23], a modified IMP via polynomial differential operator was proposed for MIMO systems. The method works well under polynomial-ordered references. However, perturbing the references or under sinusoidal references, the stability of the loop can be lost.

Considering the problems and the associated solutions reported so far, first, a natural question asks under which conditions/assumptions on the disturbance or the system could the EID definition be valid? The first contribution of the current study is the answer to the aforementioned question. We expand the theoretical analyses on the matching condition to catch the practical results of EID, which covers a wider range than theoretical results. Further, to achieve asymptotic tracking under polynomial ordered references or disturbances, a novel approach based on multiple integral augmentation and $\mathcal{H}_\infty$ based synthesis is postulated. The proposed method relaxes some limitations on the disturbances, i.e., slowly time-varying disturbances, boundedness, and thus it extends some key studies like anti-disturbance control [5] to a wider group of applications. A fundamental assumption on Hamiltonian matrices emphasizes the solvability via $\mathcal{H}_\infty$ synthesis, which is violated by the integral augmentation of the plant since no pole/zero is allowed on the imaginary-axis [24], and to the best of our knowledge, limits of the stabilizability of such systems have not been investigated for the MIMO case explicitly. Compared to the related results, the main contributions of the paper can be summarized as follows.

(a) Existence of the transformation of the unmatched disturbances to the matched ones is given analytically.
(b) Zero tracking error is achieved under unbounded polynomial-ordered disturbances as well as unknown sinusoidal disturbances.

The rest of this paper is organized as follows: Section 2 gives some fundamental definitions and assumptions about the transformation of the disturbances. Section 3 presents the analytic transformation for EID and then represents a Simplified-EID (S-EID). Section 4 presents the control system synthesis procedure and related theoretical manipulations of multiple integral augmentation regarding $\mathcal{H}_\infty$-Synthesis. Section 5 gives a comparative study and numerical results for a non-square system. Finally, Section 6 gives the concluding remarks.

2. Preliminaries

Consider the following state–space representation of a linear time-invariant system

$$\dot{x}_0(t) = \mathbf{A}x_0(t) + \mathbf{B}u(t) + \mathbf{B}_d d(t)\ ,\ \ y_0(t) = \mathbf{C}x_0(t) \tag{1}$$

where $\mathbf{A} \in \mathbb{R}^{n\times n}$, $\mathbf{B} \in \mathbb{R}^{n\times n_u}$, $\mathbf{B}_d \in \mathbb{R}^{n\times n_d}$, $\mathbf{C} \in \mathbb{R}^{n_y\times n}$, $x_0(t) \in \mathbb{R}^n$, $y_0(t) \in \mathbb{R}^{n_y}$, $u(t) \in \mathbb{R}^{n_u}$ and $d(t) \in \mathbb{R}^{n_d}$. The system above is unmatched as $\mathbf{B} \neq \mathbf{B}_d$ (so-called matching condition), and $d(t)$ is the disturbance [1,2]. The definition of EID relies on the transformation of unmatched disturbances to the matched disturbances as

$$\dot{x}(t) = \mathbf{A}x(t) + \mathbf{B}(u(t) + d_{ed}(t))\ ,\ \ y(t) = \mathbf{C}x(t). \tag{2}$$

where $d_{ed}(t)$ is the Equivalent-Input-Disturbance. In this particular context, following definition is introduced in [8,9] .

Definition 1 ([8,9]). Let the control input $u(t) = 0$ for both systems. For disturbance $d(t)$, the output of system in (1) is $y_0(t)$ and the output of system in (2) is $y(t)$ for disturbance $d_{ed}(t)$. The disturbance $d_{ed}(t)$ is called EID if $y_0(t) = y(t),\ \forall t \geq 0$.

Definition 1 is a strong definition and imposes a perfect transformation between matched disturbance and unmatched ones and using superposition principle, condition "$u(t) = 0$", which stands for simplicity, can be substituted by "$u(t)$ can be a non-zero signal if it is identical in (1) and (2)". In addition, the standard assumptions on $d(t)$ for the existence of EID are expressed as $d(t) \in L_1 \cap L_\infty$ [8] which is a very conservative condition. A relaxed yet sufficient condition on the disturbance $d(t)$ could be given by the following assumption:

Assumption 1. The disturbance $d(t)$ is a piecewise continuous function and it is of exponential order such that the Laplace transform of the disturbance exists.

Remark 1. Analyses of the following section are valid under Assumption 1. This assumption relaxes the major part of the preceding limits and suffices for control system design. However, unmatched signals, whose Laplace transforms do not exist may still be transformed into matched ones.

Without loss of generality, the initial conditions of the systems above are assumed to be zero to focus on the effect of the disturbance. Let s denote the Laplace operator, let $\mathbb{R}(s)$ denote the set of real rational transfer functions and let the Transfer Function Matrix (TFM) representation from the input $u(t)$ to the output $y_0(t)$ or from the input $u(t)$ to the output $y(t)$ be

$$\mathbf{P}(s) = \mathbf{C}(s\mathbf{I} - \mathbf{A})^{-1}\mathbf{B} = [\mathbf{P}(s)_{ij}]_{n_y\times n_u} \tag{3}$$

and the TFM representation from the disturbance $d(t)$ to the output $y_0(t)$ be

$$\mathbf{P}_{dist}(s) = \mathbf{C}(s\mathbf{I} - \mathbf{A})^{-1}\mathbf{B}_d = [\mathbf{P}_{dist}(s)_{ij}]_{n_y\times n_d} \tag{4}$$

where $\mathbf{P}(s) \in (\mathbb{R}(s)^{n_y\times n_u}, \mathbb{R}(s))$, $\mathbf{P}_{dist}(s) \in (\mathbb{R}(s)^{n_y\times n_d}, \mathbb{R}(s))$. Let $\mathbf{I}$ be the identity matrix. Each element $[\mathbf{P}(s)_{ij}]_{n_y\times n_u}$ (or $[\mathbf{P}_{dist}(s)_{ij}]_{n_y\times n_d}$) of the matrix is the individual transfer function between jth element of the $u(t)$ (or $d(t)$) and ith element of the $y(t)$ (or $y_0(t)$).

3. Existence of solutions: EID/s-EID

In this section, the necessary and sufficient conditions for exact output matching are investigated. Then, we will introduce a more practical definition of the matching condition, which is suitable for the feedback case. Note that Section 3 is seeking for answers to the following question: Under which circumstances, are we able to work with (2) (or (20) that will be introduced later) instead of (1)?.

3.1. Exact solution for EID

To show the equivalence between (1) and (2), we start with the Laplace transforms of $y_0(t)$ and $y(t)$ as

$$Y_0(s) = \mathbf{C}(s\mathbf{I} - \mathbf{A})^{-1}\mathbf{B}U(s) + \mathbf{C}(s\mathbf{I} - \mathbf{A})^{-1}\mathbf{B}_d D(s) \tag{5}$$

$$Y(s) = \mathbf{C}(s\mathbf{I} - \mathbf{A})^{-1}\mathbf{B}U(s) + \mathbf{C}(s\mathbf{I} - \mathbf{A})^{-1}\mathbf{B}D_{ed}(s) \tag{6}$$

It is noted that the Laplace transform of $d(t)$ exists due to Assumption 1 and Definition 1 implies that the output of linear time invariant (LTI) systems (5), (6) must be equal. For this equivalence, the following equalities must hold true.

$$\begin{aligned} Y(s) &= \mathbf{C}(s\mathbf{I}-\mathbf{A})^{-1}\mathbf{B}U(s) + \mathbf{C}(s\mathbf{I}-\mathbf{A})^{-1}\mathbf{B}D_{ed}(s) \\ &\triangleq \mathbf{C}(s\mathbf{I}-\mathbf{A})^{-1}\mathbf{B}U(s) + \mathbf{C}(s\mathbf{I}-\mathbf{A})^{-1}\mathbf{B}_d D(s) = Y_0(s) \\ \Rightarrow \quad & \mathbf{P}(s)D_{ed}(s) = \mathbf{P}_{dist}(s)D(s) \triangleq \mathbf{p}_d(s). \end{aligned} \tag{7}$$

Then, there exists a solution for $D_{ed}(s)$ of $\mathbf{P}(s)D_{ed}(s) = \mathbf{p}_d(s)$ if and only if

$$\text{rank}[\mathbf{P} : \mathbf{p}_d] = \text{rank}[\mathbf{P}]. \tag{8}$$

Notice that considering the vector space defined after (4) allows us to attack the problem by linear algebra. The linear equations given by (7) have a solution if and only if (8) is valid. Thus, this equation gives us the necessary and sufficient conditions.

We investigate the existence of EID (d_{ed}) (or the existence of (8)) for three cases separately, namely, (i) $n_u > n_y$, (ii) $n_u = n_y$ and (iii) $n_u \leq n_y$.

3.1.1. System has more inputs than outputs

Let $n_u > n_y$ and

$$\text{rank}[\mathbf{P}] = r \;\leq\; \min(n_y, n_u) = n_y \;\Rightarrow\; r \leq n_y \leq n_u. \tag{9}$$

The linearly independent columns of $\mathbf{P}$ could be grouped into a new matrix $\boldsymbol{\vartheta}$ as

$$\boldsymbol{\vartheta} := [\vartheta_1 \;\vartheta_2 \;\ldots\; \vartheta_r] \; s.t. \; \vartheta_{\{i=1,\ldots,r\}} \in \{\text{col}_j \mathbf{P}|_{j=1}^{n_u}\} \tag{10}$$

such that $\sum_{i=1}^{r} m_i\vartheta_i = 0$ only for $m_1 = m_2 = \cdots = m_r = 0$ where $\text{col}_j \mathbf{P} = [P_{1j}\; P_{2j} \;\ldots\; P_{n_y j}]^T$. Moreover, the spanning set of $\boldsymbol{\vartheta}$ is

$$S := \text{span}\{\vartheta_1, \vartheta_2, \ldots, \vartheta_r\} \subset \mathbb{R}(s)^{n_y \times 1}. \tag{11}$$

Therefore, there exists $x \in \mathbb{R}(s)^{n_y\times 1}$ such that $x \notin S$. So, the existence of a solution requires that

$$\mathbf{p}_d(s) \notin \mathbb{R}(s)^{n_y\times 1} \setminus S. \tag{12}$$

Now, let

$$\text{rank}[\mathbf{P}] = r \;=\; \min(n_y, n_u) = n_y \;\Rightarrow\; r = n_y \leq n_u. \tag{13}$$

Then, (10) can be rearranged as

$$\boldsymbol{\vartheta} := [\vartheta_1 \;\vartheta_2 \;\ldots\; \vartheta_{n_y}] \; s.t. \; \vartheta_{\{i=1,\ldots,n_y\}} \in \{\text{col}_j \mathbf{P}|_{j=1}^{n_u}\} \tag{14}$$

and the spanning set of $\boldsymbol{\vartheta}$ is given by $\mathbf{V} := \text{span}\{\vartheta_1, \vartheta_2, \ldots, \vartheta_{n_y}\} \subseteq \mathbb{R}(s)^{n_y\times 1}$. Since $\mathbf{p}_d(s) \in \mathbb{R}(s)^{n_y\times 1}$, $\exists \bar{m} = [\bar{m}_1 \;\bar{m}_2 \;\ldots\; \bar{m}_{n_y}] \neq 0 \; s.t. \; \mathbf{p}_d(s) = \sum_{i=1}^{n_y} \bar{m}_i\vartheta_i = 0$. Therefore,

$$\text{rank}[\mathbf{P} : \mathbf{p}_d] = \text{rank}[\mathbf{P}] \tag{15}$$

condition always satisfied. This means that there always exists a solution for $D_{ed}(s)$.

3.1.2. System is square

Let $n_u = n_y$. A system is said to be square when it has equal numbers of inputs and outputs otherwise, it is called a non-square system. Note that, all solutions given in Section 3.1.1 are valid for this case such that there always exists a solution for $D_{ed}(s)$ again. In this special case, if $\mathbf{P}^{-1}$ exists then the unique solution is

$$D_{ed}(s) = \mathbf{P}^{-1}(s)\mathbf{P}_{dist}(s)D(s). \tag{16}$$

3.1.3. System has more outputs than inputs

The third case implies that $n_y > n_u$, similar to the first case, the existence of a solution requires that

$$\mathbf{p}_d(s) \notin \mathbb{R}(s)^{n_y\times 1} \setminus \bar{S}. \tag{17}$$

where $\bar{S} := \text{span}\{\bar{\vartheta}_1, \bar{\vartheta}_2, \ldots, \bar{\vartheta}_{\bar{r}}\} \subset \mathbb{R}(s)^{n_y\times 1} \; s.t. \; \bar{r} = \text{rank}[\mathbf{P}] \leq \min(n_y, n_u) = n_u$. Moreover, to find a unique solution, if $\bar{r} = n_u$ and (17) is satisfied then $\exists \mathbf{P}^{\dagger} \; s.t. \; \mathbf{P}^{\dagger}\mathbf{P} = \mathbf{I}_{n_y\times n_y}$, where $\mathbf{P}^{\dagger} := (\mathbf{P}^T\mathbf{P})^{-1}\mathbf{P}^T$ denotes left-side pseudo-inverse of $\mathbf{P}$. Therefore, a particular solution for $D_{ed}(s)$ is obtained as

$$D_{ed}(s) = \mathbf{P}^{\dagger}(s)\mathbf{P}_{dist}(s)D(s) \tag{18}$$

To sum up, instead of considering the effects of the disturbance $d(t)$ through the $\mathbf{B}_d$ on the output $y_0(t)$, we can employ the transfer function matrix $\mathbf{P}_{dist}(s)$ whose control input is $d(t)$ and the output is $y_0(t)$. Then, in terms of transfer function matrices and signals, the aim of EID can be re-defined as searching a control input signal as $D_{ed}(s)$ for the transfer function matrix $\mathbf{P}(s)$ whose output $y(t)$ is identical to $y_0(t)$.

However, as it is stated in [9], computing $d_{ed}(t)$ exactly is complicated and also requires some future information about the outputs. Different from [9] and only for offline analysis, solving (7) under the subsequent conditions gives the exact form of the equivalent disturbances, which cannot be used directly in closed-loop systems real-time. Therefore, after checking (12) and (17), which are only possibilities of violating the existence of EID, one can focus on the design of an estimator over $d_{ed}(t)$.

Remark 2. Stable inversion problem introduced in [14], mainly summoned by the EID-based works, is a special case of the approach introduced here. This is mainly because the system given by (1)–(3) is required to be square and the time domain signals need to be bounded and integrable, which are not required in our study. Moreover, our approach only deals with the definition of EID and it does not exploit any control/observer part of the EID-estimator structure.

3.2. Simplified definition: S-EID

This subsection is dedicated to the observer design and the properties of the estimated disturbance by defining some formal conditions and performance metrics on the estimation. Therefore, instead of presenting a new type of definition about the equivalent form of the disturbances, S-EID revisits the original EID definition, which is totally valid on this study for the existence, to analytically describe the effects of the disturbance estimation on the output. The aim is to describe the observer on a rigorous mathematical base. Consider we have the $d_{ed}(t)$, which describes the polynomial-ordered disturbances in the following form. From now on, we will only deal with polynomial form of $d(t)$. The reason behind the choice of polynomial exogenous signals is due to the practical considerations, where polynomial signals are encountered much often than exponential ones.

$$d_{ed}(t) = [d_{ed,1}(t)\; d_{ed,2}(t) \;\ldots\; d_{ed,n_u}(t)]^T \text{ s.t. } d_{ed,j}(t) = \sum_{i=0}^{k_j} a_{ij}t^i \tag{19}$$

where $j = 1, \ldots, n_u$ and unknown a_{ij}, $k_j \leq \infty \; \forall i, j$ but we know a coefficient $k_j^+ \geq k_j$ that gives us a worst-case bound for the growth rate of the disturbance. Consider the following LTI system

$$\dot{\bar{x}}(t) = \mathbf{A}\bar{x}(t) + \mathbf{B}(u(t) + \bar{d}_{ed}(t)) \;,\; \bar{y}(t) = \mathbf{C}\bar{x}(t). \tag{20}$$

where the estimated disturbance $\bar{d}_{ed}$ is considered instead of true d_{ed} with the same system matrices $(\mathbf{A}, \mathbf{B}, \mathbf{C})$ of (2). Following definition enables us to design a disturbance observer such that it can be constructed by using only the measurable signals as $u(t)$ and $y(t)$.

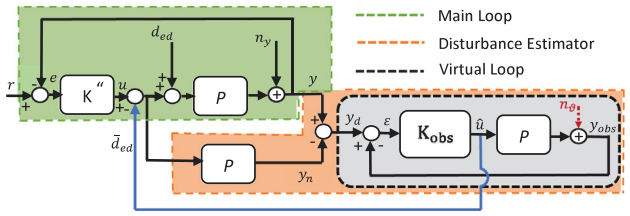

Fig. 1. The estimator configuration.

Definition 2. Let the control input $u(t)$ ensure the internal stability of (1)–(2) and (20). Then, under Assumption 1, if $\lim_{t\to\infty}(y(t) - \bar{y}(t)) = 0$ and $\|y(t) - \bar{y}(t)\|_2 = \bar{e} \leq \infty$, (i.e. $y(t) = y_0(t) \simeq \bar{y}(t)$) $\forall t \geq 0$, $\bar{d}_{ed}(t)$ is called simplified-EID (S-EID).

Note that the first part of the definition is dedicated to the unstable (yet stabilizable) systems. Without having a stabilizing control input, the design of the disturbance observer will not be helpful. Moreover, some practical problems, including the existence of measurement noise, make it hard to satisfy Definition 1. Instead of exact output matching, defining a sufficiently small $\bar{e}$ provides some robustness against the measurement noise. Therefore, Definition 2 introduces some performance metrics in a more practical way when a disturbance observer is aimed to be designed.

4. Multiple integral augmentation and $\mathcal{H}_\infty$-synthesis

In this section, with the help of Section 3, we are able to consider only the d_{ed} type of the disturbances. In addition, instead of offering a new structure for disturbance estimation, to enhance the dynamic response of the control system under polynomial-ordered disturbances, we update the design procedure of the control systems of an existing disturbance observer scheme [25]. To do it; (i) Employ multiple integral augmentation (the number of integrals can vary based on the application). (ii) Utilize bilinear transformation (note that, the augmented system includes $j\omega$-axis poles, which are infeasible for a standard $\mathcal{H}_\infty$ problem). (iii) Check the stabilizability & detectability conditions for the bilinear transformed system. (iv) Build the Linear Fractional Transformation form. (v) Minimize the lower infinity-norm bound of the closed-loop system by adjusting the bandwidth of the virtual-loop. (vi) Solve the Hamiltonian matrices to get the control system of virtual-loop. (vii) Apply inverse bilinear transformation to get a valid controller for the original (unshifted) system. (viii) Get the final form of the control system by carrying the integrator block from the plant to the controller.

Consider the estimator structure in Fig. 1. It is observed from the figure that the system has no uncertainty $\mathbf{K}_{obs}$ is a dedicated controller of the estimator loop. $\mathbf{K}$ is the main controller, $\varepsilon(t) \in \mathbb{R}^{n_y\times 1}$ is the error for the estimator loop, and $u(t) \in \mathbb{R}^{n_u\times 1}$ is the output of the main controller. The output of $\mathbf{K}_{obs}$, the estimated disturbances, is denoted as $\bar{d}_{ed}(t) := \hat{u}(t) \in \mathbb{R}^{n_u\times 1}$. The signal $r(t) \in \mathbb{R}^{n_y\times 1}$ denotes the reference signal for the overall system and $y_{obs}(t) \in \mathbb{R}^{n_y\times 1}$ is the output of the virtual loop. By equating $d_{ed}(t)$ to 0 in (2), $y_n(t)$ is obtained. The aim is to design such a $\mathbf{K}_{obs}$ that the permissible disturbance estimation error defined by Definition 2 is minimized. The relation between $\mathbf{K}_{obs}$ and the error will be introduced by Lemma 4 in the proceeding sections. Therefore, to satisfy the S-EID definition, design such a $\mathbf{K}_{obs}$ that there will be no steady-state estimation error and have a faster estimation $\bar{d}_{ed}$ providing smaller $\bar{e}$.

Proposition 1. *Based on Definition 2, the exogenous signals are in the polynomial order, which is denoted as $(k-1)$th, as $r(t)$ or $d_{ed}(t)$ lead to $y_d(t) := y(t) - y_n(t)$ that is of polynomial order.*

Proof. It is observed from (1) and (2) that the difference between $y(t)$ and $y_n(t)$ is caused only by $d_{ed}(t)$ (or equally $d(t)$) which is given by (19). Since the control input $u(t)$ is identical for both systems, we have

$$\begin{aligned}&\left[y_{dp}\right]_{n_y\times 1}\\ &= \left(\left[\mathbf{P}_{p,1}\right]_{n_y\times n_u}\left[d_{ed1}\right]_{n_u\times 1} + \cdots + \left[\mathbf{P}_{p,n_u}\right]_{n_y\times n_u}\left[d_{edn_u}\right]_{n_u\times 1}\right)\end{aligned}$$

where $p = 1, \ldots, n_y$. Assume

$$\begin{aligned}|\left[d_j\right]_{n_d\times 1}| &\leq \sum_{i=0}^{k_j} a_{ij}t^i \leq \left(a_{k_j,j}t^{k-1} + a_{k_j-1,j}t^{k-1} + \cdots + a_{0,j}t^{k-1}\right)\\ &= a'_j t^{k-1}\end{aligned} \tag{21}$$

for $j = 1, \ldots, n_u$ and $k := \max\{k_1, k_2, \ldots, k_{n_u}\} + 1$. Since we are interested in the magnitude of the disturbance in (21), we consider the coefficients of the polynomial positive, i.e. $a_{ij} \in \mathbb{R}^+$. It is straightforward to assume that the control structures $\mathbf{K}$ and $\mathbf{K}_{obs}$ must satisfy internal stability (Definition 2 provides a stabilizing $u(t)$) for their feedback loops. Then, we can define

$$\sup_{\omega\in\mathbb{R}^+}\sigma(\mathbf{P}) \leq \beta \leq \infty \text{ s.t. } \sup_{\omega\in\mathbb{R}^+}\sigma(\mathbf{P}(i,j)) \leq \bar{\beta}_{ij} \leq \beta$$

where $i = 1, \ldots, n_y$, $\bar{\sigma}$ denotes the maximum singular value of the transfer function matrix $\mathbf{P}$ and σ denotes the singular values of transfer function $\mathbf{P}(i,j)$. So, following inequalities on y_d can be written

$$\begin{aligned}\left[y_{dj}\right]_{n_y\times 1} &\leq \sum_{i=1}^{n_u}\bar{\beta}_{ji}[d_{edi}]_{n_u\times 1} \leq \sum_{i=1}^{n_u}\beta[d_{edi}]_{n_u\times 1}\\ &\leq \sum_{i=1}^{n_u}\beta a' t^{k-1} \leq \bar{K}^\star t^{k-1}\end{aligned}$$

where $a' := \max\{a'_1, \ldots, a'_{n_y}\}$, $\beta := \|\left[\bar{\beta}_{ij}\right]_{n_u\times n_y}\|_\infty$, and $\bar{K}^\star \leq \infty$ and this completes the proof. □

4.1. Disturbance observer $\mathbf{K}_{obs}$

The virtual loop shown in Fig. 1 only consists of a reference input y_d, a stabilizing controller $\mathbf{K}_{obs}$ and a nominal plant. Therefore the loop is free from disturbances (input or output). The worst-case reference input tracking occurs when $y_d(t)$ is of a polynomial order as it was described by Proposition 1. Therefore, ensuring $\varepsilon \equiv 0$ under a polynomial reference input is sufficient for all $y_d(t)$ caused by $d(t)$. To achieve this objective, first, k-fold multiple integral augmentation to the plant is performed as follows

$$\mathbf{P}_{aug} := \mathbf{P}(s)\mathbf{I}_a(s) = \left[\begin{array}{cc|c}\mathbf{A}^+ & \mathbf{0} & \mathbf{B}^+\\ \mathbf{B}\mathbf{C}^+ & \mathbf{A} & \mathbf{0}\\ \hline \mathbf{0} & \mathbf{C} & \mathbf{0}\end{array}\right] = \left[\begin{array}{c|c}\bar{\mathbf{A}} & \bar{\mathbf{B}}\\ \hline \bar{\mathbf{C}} & \bar{\mathbf{D}}\end{array}\right] \tag{22}$$

where $\mathbf{I}_a(s) := \text{diag}[\frac{1}{s^k}\ \frac{1}{s^k}\ \ldots\ \frac{1}{s^k}] = \left[\begin{array}{c|c}\mathbf{A}^+ & \mathbf{B}^+\\ \hline \mathbf{C}^+ & \mathbf{D}^+\end{array}\right]$ such that $\mathbf{I}_a(s) \in \mathbb{R}(s)^{n_u\times n_u}$. Note that the present form of (22) cannot be solved by standard $\mathcal{H}_\infty$, since it violates the fundamental principle of the synthesis. Therefore, employing the bilinear transformation approach eludes this imaginary-axis pole problem. Then, to ensure the solvability of the problem, the following assumption is made.

Assumption 2. Let $p_1, \ldots, p_n$ denote the poles of $\mathbf{P}(s)$ and $z_1, \ldots, z_m$ stand for the zeros of $\mathbf{P}(s)$ and choose sufficiently small α_1 and sufficiently large α_2 such that every p_i and z_i are included

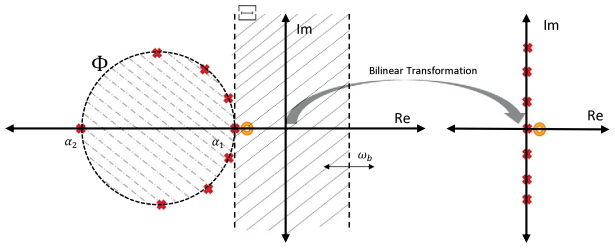

Fig. 2. Schematic limits of bilinear transformation on s-plane. The unallowable poles are red labeled (x) and unallowable zeros are orange labeled (o)-illustration.

by $\boldsymbol{\Phi}$, which is illustrated in Fig. 2.. p_i and z_i are assumed to satisfy the equalities in (23) and (24).

$$\left(\mathrm{Re}\{p_i\} - \frac{|\alpha_1+\alpha_2|}{2}\right)^2 + \mathrm{Im}\{p_i\}^2 \neq \frac{|\alpha_1-\alpha_2|^2}{4}, i = 1,\ldots,n \tag{23}$$

$$\left(\mathrm{Re}\{z_i\} - \frac{|\alpha_1+\alpha_2|}{2}\right)^2 + \mathrm{Im}\{z_i\}^2 \neq \frac{|\alpha_1-\alpha_2|^2}{4} \text{s.t. } z_i \notin \Xi, \quad \textit{for } i = 1,\ldots,m \ \square \tag{24}$$

Remark 3. The reasons behind Assumption 2 are preserving the dynamic behavior of the system and satisfying the fundamental properties of the $\mathcal{H}_\infty$-Synthesis. For instance, if (23) is violated, then we have poles on the imaginary-axis, which is not possible due to [26]. Moreover, violating (24) causes a non-existent, dominant and non-minimum phase behavior.

Under Assumption 2, applying bilinear pole-shifting [24] to $\mathbf{P}_{aug}$ yields

$$\mathbf{P}^\star_{aug} = \left[\begin{array}{c|c} (\overline{\mathbf{A}} - \alpha_1\mathbf{I})(\mathbf{I} - \frac{1}{\alpha_2}\overline{\mathbf{A}})^{-1} & (1-\frac{\alpha_1}{\alpha_2})(\mathbf{I} - \frac{1}{\alpha_2}\overline{\mathbf{A}})^{-1}\overline{\mathbf{B}} \\ \hline \overline{\mathbf{C}}(\mathbf{I} - \frac{1}{\alpha_2}\overline{\mathbf{A}})^{-1} & \overline{\mathbf{D}} + \frac{1}{\alpha_2}\overline{\mathbf{C}}(\mathbf{I} - \frac{1}{\alpha_2}\overline{\mathbf{A}})^{-1}\overline{\mathbf{B}} \end{array}\right] \tag{25}$$

Without loss of generality, under Assumption 2 for $0 > \alpha_1 \gg \alpha_2$, to reduce the computational complexity, from now on, the following equation can be used instead of (25).

$$\mathbf{P}^\star_{aug}(s) \approx \mathbf{P}(s)\mathbf{I}^+(s) = \left[\begin{array}{cc|c} \mathbf{A}_2 & \mathbf{0} & \mathbf{B}_2 \\ \mathbf{B}\mathbf{C}_2 & \mathbf{A} & \mathbf{0} \\ \hline \mathbf{0} & \mathbf{C} & \mathbf{0} \end{array}\right] = \left[\begin{array}{c|c} \mathbf{A}^\star & \mathbf{B}^\star \\ \hline \mathbf{C}^\star & \mathbf{D}^\star \end{array}\right] \tag{26}$$

where $\mathbf{I}^+(s) := \mathrm{diag}[\frac{1}{(s-\alpha_1)^k} \ \frac{1}{(s-\alpha_1)^k} \ \cdots \ \frac{1}{(s-\alpha_1)^k}] = \left[\begin{array}{c|c} \mathbf{A}_2 & \mathbf{B}_2 \\ \hline \mathbf{C}_2 & \mathbf{D}_2 \end{array}\right]$ such that $\mathbf{I}^+(s) \in \mathbb{R}(s)^{n_u \times n_u}$.

Assumption 3. $(\mathbf{A}, \mathbf{B}, \mathbf{C})$ is stabilizable and detectable.

Lemma 1. *The pairs* $(\mathbf{A}^\star, \mathbf{B}^\star)$ *and* $(\mathbf{A}^\star, \mathbf{C}^\star)$ *are stabilizable and detectable.*

Proof. The pair $(\mathbf{A}^\star, \mathbf{B}^\star)$ is stabilizable if and only if $\left[\mathbf{A}^\star - \lambda\mathbf{I} \quad \mathbf{B}^\star\right]$ has full rank for all unstable eigenvalues of $\mathbf{A}^\star$ which is denoted by λ.

Since the $\mathbf{I}^+$ has a fixed structure, $\mathbf{A}_2 := \mathrm{diag}[\Lambda_1, \ldots, \Lambda_{n_u}]$, $\mathbf{B}_2 := \mathrm{diag}[b_1, \ldots b_{n_u}]$, $\mathbf{C}_2 := \mathrm{diag}[c_1, \ldots, c_{n_u}]$ where

$$\Lambda_{(i=1,\ldots,n_u)} = \begin{bmatrix} \alpha_1 & 1 & 0 & \ldots & 0 \\ 0 & \alpha_1 & 1 & \ldots & 0 \\ 0 & 0 & \ddots & \ldots & \vdots \\ 0 & 0 & \ldots & \alpha_1 & 1 \\ 0 & 0 & \ldots & 0 & \alpha_1 \end{bmatrix}_{[k\times k]}, \tag{27}$$

$b_1 = b_2 = \cdots = b_{n_u} = [0\ 0\ \ldots\ \star]^T_{[k\times 1]}$,
$c_1 = c_2 = \cdots = c_{n_u} = [\star\ 0\ \ldots\ 0]_{[1\times k]}$.
First, let $\lambda \in \mathrm{eig}(\mathbf{A}) \backslash \mathrm{eig}(\mathbf{A}_2)$. Then, the column rank condition for stabilizability is

$$\begin{aligned} \mathrm{rank}\,\mathbf{M} &= \mathrm{rank}\begin{bmatrix} \mathbf{A}_2 - \lambda\mathbf{I} & \mathbf{0} & \mathbf{B}_2 \\ \mathbf{B}\mathbf{C}_2 & \mathbf{A} - \lambda\mathbf{I} & \mathbf{0} \end{bmatrix} \\ &= \mathrm{rank}\left[\begin{array}{cc:c} \mathbf{A}_2 - \lambda\mathbf{I} & \mathbf{B}_2 & \mathbf{0} \\ \mathbf{B}\mathbf{C}_2 & \mathbf{0} & \mathbf{A} - \lambda\mathbf{I} \end{array}\right] \\ &= \mathrm{rank}\left[\begin{array}{c:c} \mathbf{A}' & \mathbf{B}' \\ \mathbf{C}' & \mathbf{D}' \end{array}\right] \end{aligned} \tag{28}$$

Note that, $\mathbf{A}'$ is nonsingular and $\mathcal{N}(\mathbf{B}') \subseteq \mathcal{N}(\mathbf{A}') = 0$ where $\mathcal{N}(.)$ denotes the null-space. Consider the Aitken block-diagonalization formula [27] as

$$\begin{bmatrix} \mathbf{I} & \mathbf{0} \\ -\mathbf{C}'(\mathbf{A}')^{-1} & \mathbf{I} \end{bmatrix}\begin{bmatrix} \mathbf{A}' & \mathbf{B}' \\ \mathbf{C}' & \mathbf{D}' \end{bmatrix}\begin{bmatrix} \mathbf{I} & -(\mathbf{A}')^{-1}\mathbf{B}' \\ \mathbf{0} & \mathbf{I} \end{bmatrix} = \begin{bmatrix} \mathbf{A}' & \mathbf{0} \\ \mathbf{0} & \mathbf{M}/\mathbf{A}' \end{bmatrix}$$

where $\mathbf{M}/\mathbf{A}' = \mathbf{D}' - \mathbf{C}'(\mathbf{A}')^{-1}\mathbf{B}'$. Then, by using Guttman rank additivity [27], following rank relations can be derived.

$$\begin{aligned} \mathrm{rank}[\mathbf{M}] &= \mathrm{rank}[\mathbf{A}_2] + \mathrm{rank} \\ &\quad \times \left[[\mathbf{0} \quad \mathbf{A} - \lambda\mathbf{I}] - [(\mathbf{B}\mathbf{C}_2)(\mathbf{A}_2 - \lambda\mathbf{I})^{-1}(\mathbf{B}_2 \quad \mathbf{0})]\right] \\ &= \mathrm{rank}[\mathbf{A}_2] + \mathrm{rank}[-\mathbf{B}\mathbf{C}_2(\mathbf{A}_2 - \lambda\mathbf{I})^{-1}\mathbf{B}_2 \,\vdots\, (\mathbf{A} - \lambda\mathbf{I})] \\ &= \mathrm{rank}[\mathbf{A}_2] + \mathrm{rank}\left[-\frac{1}{(\lambda-\alpha_1)^k}\mathbf{B} \,\vdots\, (\mathbf{A} - \lambda\mathbf{I})\right] \end{aligned} \tag{29}$$

and since $(\mathbf{A}, \mathbf{B})$ is stabilizable (by Assumption 3), we get

$$\mathrm{rank}[\mathbf{M}] = \mathrm{rank}[\mathbf{A}'] + \mathrm{rank}[\mathbf{D}' - \mathbf{C}'(\mathbf{A}')^{-1}\mathbf{B}'] = (n_u \times k) + n \tag{30}$$

Now, let $\lambda = \alpha_1 \in \mathrm{eig}(\mathbf{A}_2)$ and $\lambda \notin \mathrm{eig}(\mathbf{A})$. Rewriting (28) yields

$$\mathrm{rank}[\mathbf{M}] = \mathrm{rank}[\mathbf{D}'] + \mathrm{rank}[\mathbf{A}'] \tag{31}$$

where $\mathbf{A}' = [\mathbf{A}_2 - \lambda\mathbf{I} \quad \mathbf{B}_2]$, $\mathbf{B}' = \mathbf{0}$, $\mathbf{C}' = [\mathbf{B}\mathbf{C}_2 \quad \mathbf{0}]$, $\mathbf{D}' = [\mathbf{A} - \lambda\mathbf{I}]$ such that $\exists(\mathbf{D}')^{-1}$. Since $\dim[\ker(\mathbf{A}_2 - \lambda\mathbf{I})] = n_u$ and using (27), we get

$$\begin{aligned} &\mathrm{rank}[\mathbf{A}_2 - \lambda\mathbf{I}] = (n_u \times k) - n_u \qquad (32) \\ &\mathrm{rank}[\mathbf{A}'] = \mathrm{rank}\Big[[\mathbf{A}_2 - \lambda\mathbf{I} \quad \mathbf{B}_2]\Big] = (n_u \times k) \\ &\mathrm{rank}[\mathbf{D}'] = n \Rightarrow \mathrm{rank}[\mathbf{M}] = n + (n_u \times k)\,. \end{aligned}$$

The detectability property is the dual of stabilizability and this completes the proof. $\square$

Then, lower LFT based on the scheme given by Fig. 3 is employed where $\mathbf{K}_{obs}$ denotes the control system of the bilinear transformed $\mathbf{P}^\star_{aug}$, $\mathbf{W}_{P,obs}$ denotes the performance weight $\mathbf{W}_{U,obs}$ denotes input usage weight.

A possible way to define $\mathbf{W}_{P,obs}$ is [26]

$$\mathbf{W}_{P,obs}(s) = \mathrm{diag}\left[\left(\frac{\frac{s}{\sqrt[k_p]{M_p}} + \omega_{b,1}}{s + \omega_{b,1}\sqrt[k_p]{\xi_p}}\right)^{k_p} \ \ldots \ \left(\frac{\frac{s}{\sqrt[k_p]{M_p}} + \omega_{b,n_y}}{s + \omega_{b,n_y}\sqrt[k_p]{\xi_p}}\right)^{k_p}\right] \tag{33}$$

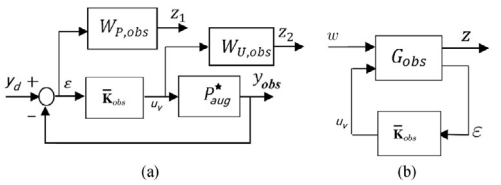

Fig. 3. LFT of the virtual loop.

where ω_b is a cut-off frequency for the sensitivity function, M_p is the maximum allowable overshoot for $\mathbf{W}_{P,obs}$ and integer $k_p > k$. The estimation error of the disturbance $(d_{ed} - \bar{d}_{ed})$ can be seen as a decreasing function of the cut-off frequency ω_b and the low-frequency roll-off rate of $\mathbf{W}_{P,obs}$. Thus, increasing ω_b or low-frequency roll-off rate can decrease $d_{ed} - \bar{d}_{ed}$.

A general form for the weight $\mathbf{W}_{U,obs}$ is

$$\mathbf{W}_{U,obs}(s) = \text{diag}\left[\left(\frac{s+\omega_{\vartheta c}/\sqrt[k_u]{M_u}}{s\sqrt[k_u]{\xi_u}+\omega_{\vartheta c}}\right)^{k_u} \cdots \left(\frac{s+\omega_{\vartheta c}/\sqrt[k_u]{M_u}}{s\sqrt[k_u]{\xi_u}+\omega_{\vartheta c}}\right)^{k_u}\right] \tag{34}$$

where $\omega_{\vartheta c}$ is cut-off frequency for $\bar{\mathbf{K}}_{obs}(\mathbf{I}+\mathbf{P}^{\star}_{aug}\bar{\mathbf{K}}_{obs})^{-1}$, M_u is the maximum permissible input usage for $\bar{\mathbf{K}}_{obs}(\mathbf{I}+\mathbf{P}^{\star}_{aug}\bar{\mathbf{K}}_{obs})^{-1}\varepsilon$, $\xi_u \ll 1$ to prevent high frequency control input usage and k_u is some integer greater than 1.

Then, although the virtual-loop (as disturbance observer) does not have any measurement noise naturally, still the noise of the main loop must be considered in the design of the virtual loop. The reason is that it is hard to distinguish between disturbance, which should be rejected, and noise, which should not be compensated, by observing just the output and input of the system with the disturbance observer. Thus, the measurement noise n_y in Fig. 1 can be carried to the output of the virtual-loop by equating $n_y = -n_\vartheta$. Note that measurement noise has high frequencies and is typically zero-mean [28]. This transportation is done virtually and only for the design/analysis of the $\bar{\mathbf{K}}_{obs}$. Then, consider $\frac{\bar{D}_{ed}(s)}{N_v(s)} := \bar{\mathbf{K}}_{obs}(\mathbf{I}+\mathbf{P}^{\star}_{aug}\bar{\mathbf{K}}_{obs})^{-1}$ which is a transfer function matrix from the n_ϑ to the $\bar{d}_{ed}$. The design aim is shaping this special TFM so-called noise sensitivity function for smooth control input (or equivalently, disturbance estimation) that has not been affected by measurement noise. To do so, we introduced the weight $\mathbf{W}_{U,obs}$. Using (34), a schematic way for $\mathbf{W}_{U,obs}$ selection (for disturbance observer design particularly) can be represented by Fig. 4 where γ denotes the infinite norm of the closed-loop system, $\bar{\sigma}\left(\mathbf{W}_{U,obs}\right)^{-1}\left(\underline{\sigma}\left(\mathbf{W}_{U,obs}\right)^{-1}\right)$ denotes the maximum (minimum) singular value of the inverse of $\mathbf{W}_{U,obs}$ and the regions of "Disturbance Estimation" and "Noise Reduction" are forbidden zones. In addition, the frequencies higher than $\omega_{\vartheta c}$ can be considered as noise dominant region, smaller than $\omega_{\vartheta c}$ can be considered as disturbance dominant region. The selection of the $\omega_{\vartheta c}$ can vary based on the measurement sensor's dynamics and disturbance profile. For further discussions about weight selection, see [29].

The representation of the augmented plant $\mathbf{G}_{obs}$ is

$$\mathbf{G}_{obs}(s) = \left[\begin{array}{c|c} \mathbf{W}_{P,obs} & -\mathbf{W}_{P,obs}\mathbf{P}^{\star}_{aug} \\ \mathbf{0} & \mathbf{W}_{U,obs} \\ \hline \mathbf{I} & -\mathbf{P}^{\star}_{aug} \end{array}\right] = \left[\begin{array}{c|c} \mathbf{G}_{11}(s) & \mathbf{G}_{12}(s) \\ \hline \mathbf{G}_{21}(s) & \mathbf{G}_{22}(s) \end{array}\right]$$
$$= \left[\begin{array}{c|c} \mathbf{A}_g & \mathbf{B}_g \\ \hline \mathbf{C}_g & \mathbf{D}_g \end{array}\right] = \left[\begin{array}{c|cc} \mathbf{A}_g & \mathbf{B}_{g,1} & \mathbf{B}_{g,2} \\ \hline \mathbf{C}_{g,1} & \mathbf{D}_{g,11} & \mathbf{D}_{g,12} \\ \mathbf{C}_{g,2} & \mathbf{D}_{g,21} & \mathbf{D}_{g,22} \end{array}\right] \tag{35}$$

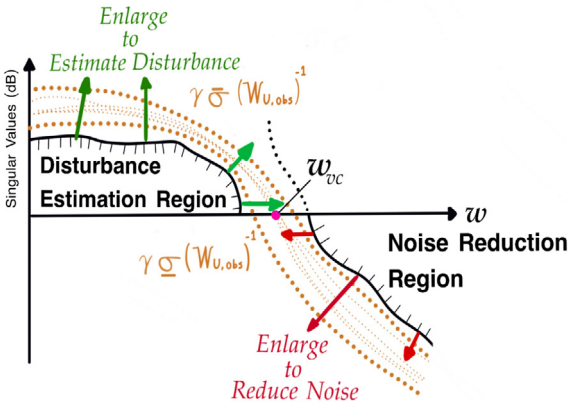

Fig. 4. A schematic way for $\mathbf{W}_{U,obs}$ selection.

and the transfer function matrix from w to z in Fig. 3 as in lower LFT form is

$$\bar{\mathbf{T}}_{obs} = \mathcal{F}_l(\mathbf{G}_{obs}, \bar{\mathbf{K}}_{obs}) = \mathbf{G}_{11} + \mathbf{G}_{12}\bar{\mathbf{K}}_{obs}(\mathbf{I}-\mathbf{G}_{22}\bar{\mathbf{K}}_{obs})^{-1}\mathbf{G}_{21}$$

The aim is to design a $\bar{\mathbf{K}}_{obs}$ that satisfies the following expression if it is feasible.

$$\|\mathcal{F}_l(\mathbf{G}_{obs}, \bar{\mathbf{K}}_{obs})\|_\infty = \|\bar{\mathbf{T}}_{obs}\|_\infty \le \gamma \le \infty \tag{36}$$

Due to the nature of the integral augmentation and (36) requires no unstable pole/zero cancellation, $\bar{\mathbf{T}}_{obs}$ always contains one or more unstable poles at the same point (i.e., $p = \alpha_1 + j0$), thus, the following lemma is immediately necessary, particularly for many RHP poles.

Lemma 2. *The complementary sensitivity function of the virtual loop satisfies the following inequality*

$$\log\|\bar{\mathbf{T}}_{obs}\|_\infty \ge \frac{k\left((2\theta_p - \pi)\log(\frac{\omega_c}{\sigma_p})\right) + \tilde{I}(\theta_p)}{2\theta_p} \tag{37}$$

where

$$\theta_p = \tan^{-1}\frac{\omega_c}{\sigma_p}\,,\ \tilde{I}(\theta) = \frac{1}{2}\left(-\int_0^{2\theta}\log(2\sin\frac{z}{2})dz - \int_0^{\pi-2\theta}\log(2\sin\frac{z}{2})dz\right)$$

Proof. First note that, any complementary sensitivity function can be modeled as

$$\bar{\sigma}(\bar{\mathbf{T}}_{obs}(j\omega)) \le (\frac{\omega_c}{\omega})^k,\ \bar{\mathbf{T}}_{obs} \in \mathbb{C}^{n_y \times n_y} \tag{38}$$

where $\mathbb{C}$ denotes the set of complex numbers and by definition $\bar{\mathbf{T}}_{obs,ij} \approx 0$ for $i \ne j$. We can define multiple cut-off frequencies for $\bar{\mathbf{T}}_{obs,ii}, i = 1,\ldots,n_y$ as $\omega_{c1},\ldots,\omega_{cn_y}$ and define $\omega_c = \min\{\omega_{c1},\ldots,\omega_{cn_y}\}$. For simplicity, we only consider RHP poles of shifted-augmented integrals and with the help of Assumption 2, we can assume that there are no RHP zeros. Now, consider the unstable poles are given by $p = \sigma_p + j\omega_p$ and then set $\omega_p = 0, \sigma_p = \alpha_1$ caused by the bilinear transformation as $p = \sigma_p$ and $\bar{p} = \sigma_p$ and thus $\theta_p = \tan^{-1}(\frac{\omega}{\sigma_p}) = \bar{\theta}_p \in [0, \pi/2]$ and $\frac{d\theta_p}{d\omega} = \frac{\sigma_p}{\sigma_p^2+\omega^2}$.

Then noting Theorem 4.2 with (4.14) in [30] and using (38) yields

$$0 \le \int_{-\infty}^{\infty} \log\bar{\sigma}(\bar{\mathbf{T}}_{obs}(j\omega))d\theta_p = 2\int_{0}^{\infty} \log\bar{\sigma}(\bar{\mathbf{T}}_{obs}(j\omega))d\theta_p$$
$$= 2\int_{0}^{\omega_c} \log\bar{\sigma}(\bar{\mathbf{T}}_{obs}(j\omega))d\theta_p + 2\int_{\omega_c}^{\infty} \log\bar{\sigma}(\bar{\mathbf{T}}_{obs}(j\omega))d\theta_p$$
$$\le 2\log\|\bar{\mathbf{T}}_{obs}\|_\infty[\theta_p(\omega_c) - \theta_p(0)] + (-2k_p)\int_{\omega_c}^{\infty} \log\frac{\omega}{\omega_c}d\theta_p.$$

Then following Theorem 2 in [31] completes proof. □

Corollary 1. *The adverse effects of adding RHP poles to the bound of the complementary sensitivity function of the bilinear transformed system can be reduced (or eliminated totally) by increasing the cut-off frequency ω_c.*

Proof. For the increasing values of ω_c with constant σ_p, the convergent rate of the $\tan^{-1}\left((\frac{\omega_c}{\sigma_p})\right)$ function to the π is higher than the divergent rate of the $k\log\left((\frac{\omega_c}{\sigma_p})\right)$. In addition, for the second term of the right side of the (37), $\tilde{I}(\theta_p)$ is positive but a decreasing function of ω_c merely since the RHP poles are real and have the constant position. Therefore, $\lim_{\omega_c\to\infty} k\left((2\theta_p - \pi)\log(\frac{\omega_c}{\sigma_p})\right) = 0$ and $\lim_{\omega_c\to\infty}\tilde{I}(\theta_p) = 0 + \epsilon$ for some positive $\epsilon \to 0$, which complete proof. □

The developed analyses up to now allow to consider the solvability of the problem with standard $\mathcal{H}_\infty$-Synthesis as its current form (36). The following theorem combining Section 1, Theorem 2.1 and Theorem 3.1 of [32] about Schur–Hamiltonian Decomposition is utilized.

Theorem 1. *Let* $\bar{\mathbf{M}} = \begin{bmatrix}\mathbf{F}^1 & \mathbf{N}^1\\ \mathbf{Z}^1 & -\mathbf{F}^1\end{bmatrix}$ *is Hamiltonian and there is no eigenvalue of* $\bar{\mathbf{M}}$ *on the jω-axis. Then there exists a unitary* $\mathbf{Q}^1 = \begin{bmatrix}\mathbf{Q}^1_{11} & \mathbf{Q}^1_{12}\\ -\mathbf{Q}^1_{12} & \mathbf{Q}^1_{11}\end{bmatrix} \in \mathbb{C}^{2n\times 2n}$ *where* $\mathbf{Q}^1_{11}, \mathbf{Q}^1_{12} \in \mathbb{C}^{n\times n}$ *such that* $(\mathbf{Q}^1)^T\bar{\mathbf{M}}\mathbf{Q}^1 = \begin{bmatrix}\mathbf{T}^1 & \mathbf{R}^1\\ \mathbf{0} & -\mathbf{T}^1\end{bmatrix}$ *where* $\mathbf{T}^1, \mathbf{R}^1 \in \mathbb{C}^{n\times n}$, $\mathbf{R}^1 = (\mathbf{R}^1)^T$, $\mathbf{T}^1$ *is upper triangular. In this discussion,* $\mathbf{Q}^1$ *can be chosen such that* $\mathbf{T}^1 \in \mathbb{C}_-$ *and also it satisfies*

$$\begin{bmatrix}\mathbf{F}^1 & \mathbf{N}^1\\ \mathbf{Z}^1 & -\mathbf{F}^1\end{bmatrix}\begin{bmatrix}\mathbf{Q}^1_{11}\\ -\mathbf{Q}^1_{12}\end{bmatrix} = \begin{bmatrix}\mathbf{Q}^1_{11}\\ -\mathbf{Q}^1_{12}\end{bmatrix}\mathbf{T}^1 \equiv \begin{bmatrix}\hat{\mathbf{F}}^1 & \hat{\mathbf{N}}^1\\ \hat{\mathbf{Z}}^1 & -\hat{\mathbf{F}}^1\end{bmatrix}\begin{bmatrix}\Sigma^1\\ -\Delta^1\end{bmatrix}$$
$$= \begin{bmatrix}\Sigma^1\\ -\Delta^1\end{bmatrix}\hat{\mathbf{T}}^1 \tag{39}$$

where, using symplectic singular value decomposition, there exist $n\times n$ *unitary matrices* $\mathbf{U}$ *and* $\mathbf{V}$ *such that* $\mathbf{U}^T\mathbf{Q}^1_{11}\mathbf{V} = \Sigma^1 = \mathrm{diag}(\sigma_1,\ldots,\sigma_n)$, $0 \le \sigma_1 \le \cdots \le \sigma_n$, $\mathbf{U}^T\mathbf{Q}^1_{12}\mathbf{V} = \Delta^1 = \mathrm{diag}(\delta_1,\ldots,\delta_n)$, $\delta_i = \pm(1-\sigma_i^2)^{1/2}$, $\hat{\mathbf{F}}^1 = \mathbf{U}^T\mathbf{F}^1\mathbf{U}$, $\hat{\mathbf{N}}^1 = \mathbf{U}^T\mathbf{N}^1\mathbf{U}$, $\hat{\mathbf{Z}}^1 = \mathbf{U}^T\mathbf{Z}^1\mathbf{U}$ *and* $\hat{\mathbf{T}}^1 = \mathbf{V}^T\mathbf{T}^1\mathbf{V}$. *Define the Algebraic Riccati Equations as*

$$-\mathbf{X}\mathbf{N}^1\mathbf{X} + \mathbf{X} + (\mathbf{A}^1)^T\mathbf{X} + \mathbf{Z}^1 = \mathbf{0} \tag{40}$$
$$-\hat{\mathbf{X}}\hat{\mathbf{N}}^1\hat{\mathbf{X}} + \hat{\mathbf{X}} + (\hat{\mathbf{A}}^1)^T\hat{\mathbf{X}} + \hat{\mathbf{Z}}^1 = \mathbf{0} \tag{41}$$

where $\mathbf{X} = \mathbf{U}\hat{\mathbf{X}}\mathbf{U}^T$ *and* $\hat{\mathbf{X}} = \mathrm{diag}(\delta_1/\sigma_1,\ldots,\delta_n/\sigma_n)$ *are the Hermitian solutions of (40) and (41) respectively. Then,* $\sigma_1 \neq 0$ *implies that there exists a positive semi-definite diagonal matrix* $\mathbf{X}$.

Proof. See [32] □

Then, describe the Hamiltonian matrices as in (42) and (43)

$$H^1_\infty = \left[\begin{array}{c:c}\mathbf{F}^1 & \mathbf{N}^1\\ \hdashline \mathbf{Z}^1 & -\mathbf{F}^1\end{array}\right] \tag{42}$$

$$J^1_\infty = \begin{bmatrix}\mathbf{A}_g & \mathbf{0}\\ -\mathbf{B}_{g,1}\mathbf{B}^T_{g,1} & -\mathbf{A}_g\end{bmatrix} - \begin{bmatrix}[\mathbf{C}_{g,1}\ \mathbf{C}_{g,2}]\\ -\mathbf{B}_{g,1}[\mathbf{D}_{g,11}\ \mathbf{D}_{g,21}]\end{bmatrix}$$
$$\times\bar{\mathbf{R}}^{-1}\begin{bmatrix}\mathbf{D}_{g,11}\\ \mathbf{D}_{g,21}\end{bmatrix}\mathbf{B}^T_{g,1}\begin{bmatrix}\mathbf{C}_{g,1}\\ \mathbf{C}_{g,2}\end{bmatrix} \tag{43}$$

where $\mathbf{F}^1 = \mathbf{A}_g + [\mathbf{B}_{g,1}\ \mathbf{B}_{g,2}]\mathbf{R}^{-1}\begin{bmatrix}\mathbf{D}_{g,11}\\ \mathbf{D}_{g,12}\end{bmatrix}\mathbf{C}_{g,1}$, $\mathbf{N}^1 = -[\mathbf{B}_{g,1}\ \mathbf{B}_{g,2}]\mathbf{R}^{-1}[\mathbf{B}_{g,1}\ \mathbf{B}_{g,2}]^T$, $\mathbf{Z}^1 = -\mathbf{C}^T_{g,1}\left(\mathbf{I} + [\mathbf{D}_{g,11}\ \mathbf{D}_{g,12}]\mathbf{R}^{-1}\begin{bmatrix}\mathbf{D}_{g,11}\\ \mathbf{D}_{g,12}\end{bmatrix}\right)\mathbf{C}_{g,1}$, $\mathbf{F}^1 = \left(\mathbf{A}_g + [\mathbf{B}_{g,1}\ \mathbf{B}_{g,2}]\mathbf{R}^{-1}\begin{bmatrix}\mathbf{D}_{g,11}\\ \mathbf{D}_{g,12}\end{bmatrix}\mathbf{C}_{g,1}\right)^T$, $\mathbf{R} = \begin{bmatrix}\mathbf{D}_{g,11}\\ \mathbf{D}_{g,12}\end{bmatrix}[\mathbf{D}_{g,11}\ \mathbf{D}_{g,12}] - \begin{bmatrix}\gamma^2\mathbf{I} & \mathbf{0}\\ \mathbf{0} & \mathbf{0}\end{bmatrix}$ and $\bar{\mathbf{R}} = \begin{bmatrix}\mathbf{D}_{g,11}\\ \mathbf{D}_{g,21}\end{bmatrix}[\mathbf{D}_{g,11}\ \mathbf{D}_{g,21}] - \begin{bmatrix}\gamma^2\mathbf{I} & \mathbf{0}\\ \mathbf{0} & \mathbf{0}\end{bmatrix}$.

From now on, we only consider H^1_∞ Hamiltonian matrix. To get $\mathbf{G}^0_{obs}$, $\mathbf{P}^\star_{aug}$ is replaced with $\mathbf{P}$ in (35) and following (36), (42), (43) yields for the unaugmented system's Hamiltonian matrices H^0_∞ and J^0_∞ respectively.

Assumption 4. The systems defined by $\mathbf{G}_{obs}$ and $\mathbf{G}^0_{obs}$ satisfy A1–A6 from [33]. Then, assume that $H^0_\infty \in \mathrm{dom}(\mathrm{Ric})$ and $\mathrm{Ric}(H^0_\infty) = \mathbf{X}^0 \ge 0$ where dom(Ric) denotes Riccati Domain that is defined by all-Hamiltonian matrices which have no pole/zero on their imaginary-axis and there exist non-singular bases for stable invariant subspace of the corresponding Hamiltonian matrix.

Theorem 2. *If there exist* $\mathbf{X}^0 \ge 0$ *satisfying Theorem 1 and Assumption 4, then* $\exists\mathbf{X} \ge 0$ *that satisfies (40) for* H^1_∞ *Hamiltonian matrix.*

Proof. Reorganize Σ^1 and Δ^1 as

$$\Sigma^1 = \begin{bmatrix}\Sigma^1_1 & \mathbf{0}\\ \mathbf{0} & \Sigma^1_2\end{bmatrix},\ \Delta^1 = \begin{bmatrix}\Delta^1_1 & \mathbf{0}\\ \mathbf{0} & \Delta^1_2\end{bmatrix} \tag{44}$$

and suppose

$$0 = \sigma_1 = \cdots = \sigma_i \le \sigma_{i+1} \tag{45}$$
$$\Sigma^1_1 = \mathrm{diag}(\sigma_1,\ldots,\sigma_i) = \mathbf{0} \tag{46}$$
$$\Sigma^1_2 = \mathrm{diag}(\sigma_{i+1},\ldots,\sigma_n)\ s.t.\ \exists(\Sigma^1_2)^{-1} \tag{47}$$
$$\therefore \Delta^1_1 = \mathrm{diag}(\delta_1,\ldots,\delta_i) = \mathbf{I}_{i\times i} \tag{48}$$

for some $i \le n$. Note that (45) violates the existence of $\mathbf{X}$. Using (44), reorganizing (39) yields

$$\begin{bmatrix}\hat{\mathbf{F}}^1_{11} & \hat{\mathbf{F}}^1_{12} & \hat{\mathbf{N}}^1_{11} & \hat{\mathbf{N}}^1_{12}\\ \hat{\mathbf{F}}^1_{21} & \hat{\mathbf{F}}^1_{22} & \hat{\mathbf{N}}^1_{21} & \hat{\mathbf{N}}^1_{22}\\ \hat{\mathbf{Z}}^1_{11} & \hat{\mathbf{Z}}^1_{12} & -\hat{\mathbf{F}}^1_{11} & -\hat{\mathbf{F}}^1_{21}\\ \hat{\mathbf{Z}}^1_{21} & \hat{\mathbf{Z}}^1_{22} & -\hat{\mathbf{F}}^1_{12} & -\hat{\mathbf{F}}^1_{22}\end{bmatrix}\begin{bmatrix}\Sigma^1_1 & \mathbf{0}\\ \mathbf{0} & \Sigma^1_2\\ \mathbf{I}_{i\times i} & \mathbf{0}\\ \mathbf{0} & -\Delta^1_2\end{bmatrix} = \begin{bmatrix}\Sigma^1_1 & \mathbf{0}\\ \mathbf{0} & \Sigma^1_2\\ \mathbf{I}_{i\times i} & \mathbf{0}\\ \mathbf{0} & -\Delta^1_2\end{bmatrix}$$
$$\times\begin{bmatrix}\hat{\mathbf{T}}^1_{11} & \hat{\mathbf{T}}^1_{12}\\ \hat{\mathbf{T}}^1_{21} & \hat{\mathbf{T}}^1_{22}\end{bmatrix}.$$

By comparing (1,1) blocks in the equation, we find that $\hat{\mathbf{N}}^1_{11} = 0$. Then,

$$\hat{\mathbf{N}}^1_{11} = \begin{bmatrix}1 & 0 & \ldots & 0 & 0\\ 0 & 0 & \ldots & 0 & 1\end{bmatrix}^T\hat{\mathbf{N}}^0_{11}\begin{bmatrix}* & 0 & \ldots & 0\\ 0 & 0 & \ldots & *\end{bmatrix} \tag{49}$$

where $* \neq 0 \in \mathbb{R}$. Reorganizing H^0_∞ in (49) and using Assumption 4 show that $\Sigma^0 \neq 0$ and $\hat{\mathbf{N}}^0_{11} \neq 0$ therefore $\hat{\mathbf{N}}^1_{11} \neq 0$, which is a contradiction. Thus, $\Sigma^1_1 \neq 0$ and following Theorem 1, (40) and (41) gives $\mathbf{X} \ge 0$. □

Then, following the design procedure described in [33] yields an admissible control system, which satisfies (36) and the structure of the control system is given by $\bar{\mathbf{K}}_{obs} = \left[\begin{array}{c|c}\bar{\mathbf{A}}_{co} & \bar{\mathbf{B}}_{co}\\ \hline \bar{\mathbf{C}}_{co} & \bar{\mathbf{D}}_{co}\end{array}\right]$.

Now, the below inverse bilinear transformation procedure should be applied to $\bar{\mathbf{K}}_{obs}$ to get a realizable control system.

$$\tilde{\mathbf{K}}_{obs} = \left[\begin{array}{c|c} (-\bar{\mathbf{A}}_{co} - \alpha_1\mathbf{I})(-\mathbf{I} - \frac{1}{\alpha_2}\bar{\mathbf{A}}_{co})^{-1} & (1-\frac{\alpha_1}{\alpha_2})(-\mathbf{I} - \frac{1}{\alpha_2}\bar{\mathbf{A}}_{co})^{-1}\bar{\mathbf{B}}_{co} \\ \hline \bar{\mathbf{C}}_{co}(-\mathbf{I} - \frac{1}{\alpha_2}\bar{\mathbf{A}}_{co})^{-1} & \bar{\mathbf{D}}_{co} + \frac{1}{\alpha_2}\bar{\mathbf{C}}_{co}(-\mathbf{I} - \frac{1}{\alpha_2}\bar{\mathbf{A}}_{co})^{-1}\bar{\mathbf{B}}_{co} \end{array}\right] \tag{50}$$

Final form of $\mathbf{K}_{obs}$ is obtained as follows.

$$\mathbf{K}_{obs}(s) = \tilde{\mathbf{K}}_{obs}(s)\mathbf{I}_a(s). \tag{51}$$

Similar to [24], the following inequalities show that the control system designed using the bilinear transformed augmented plant has better infinity norm characteristics after inverse bilinear transformation.

$$\begin{aligned} \gamma &> \|\mathcal{F}_l(\mathbf{G}_{obs}, \bar{\mathbf{K}}_{obs})(j\tilde{\omega})\|_\infty = \sup_{\tilde{\omega}} \bar{\sigma}(\mathcal{F}_l(\mathbf{G}_{obs}, \bar{\mathbf{K}}_{obs})(j\tilde{\omega})) \\ &= \sup_{\mathbb{R}(\tilde{s})>0} \bar{\sigma}(\mathcal{F}_l(\mathbf{G}_{obs}, \bar{\mathbf{K}}_{obs})(\tilde{s})) \\ &\geq \sup_{s\in\mathbb{C}\setminus\Omega} \bar{\sigma}(\mathcal{F}_l(\mathbf{G}_{obs}, \bar{\mathbf{K}}_{obs})(\frac{s-\alpha_1}{1-\frac{s}{\alpha_2}})) = \sup_{s\in\mathbb{C}\setminus\Omega} \bar{\sigma}\mathcal{F}_l(\mathbf{G}^0_{obs}, \mathbf{K}_{obs})(s) \\ &\geq \lim_{s\to j\omega} \sup_{\omega} \mathcal{F}_l(\mathbf{G}^0_{obs}, \mathbf{K}_{obs})(j\omega). \end{aligned} \tag{52}$$

Lemma 3. *According to (36) and (52), for polynomial order $y_d(t)$, the steady-state error of the virtual loop will be zero.*

Proof. Noting properties (1-3) from [24] with $\boldsymbol{\mathcal{S}}$

$$\boldsymbol{\mathcal{S}}^{out}_{obs}(s) := \begin{bmatrix} \mathcal{S}^{out}_{obs\,1,1} & \cdots & \mathcal{S}^{out}_{obs\,1,n_y} \\ \vdots & \ddots & \vdots \\ \mathcal{S}^{out}_{obs\,n_y,1} & \cdots & \mathcal{S}^{out}_{obs\,n_y,n_y} \end{bmatrix} = (\mathbf{I} + \mathbf{P}\mathbf{K}_{obs})^{-1} \in \mathcal{RH}_\infty$$

where $\mathcal{S}^{out}_{obs}(i,j) = gs^k\left(\prod_{m=1}^{n-k}(s-a_m)\right)\left(\prod_{m=1}^{n}(s-b_m)\right)^{-1}$, g is the appropriate gain of the corresponding minor and $a_m, b_m \in \mathbb{C}$, $\forall m$ and these are functions of i and j for $i = 1,\ldots,n_y, j = 1,\ldots,n_y$. Then using the final value theorem as $\lim_{s\to 0}(s\mathbf{S}^{out}_{obs}(s)Y_d(s))$ with Proposition 1 completes the proof. □

Lemma 4. *The estimation* performance *of the observer can be specified by the input complementary sensitivity function of the virtual loop $\mathbf{T}^{inp}_{obs}$. Specifically*

$$\hat{u} := \bar{d}_{ed} = \mathbf{T}^{inp}_{obs} d_{ed}\ . \tag{53}$$

Proof. Similar with the proof of Lemma 1 in [34]. □

Corollary 2. *The harmonic components of the disturbance whose $(k+1)$-fold derivatives are not constant or zero are directly compensated by enlarging the bandwidth of the observer's controller.*

Proof. Consider (31) in [35] as

$$d(t) = \beta_1 \sin(\omega_1 t + \gamma_1)$$

Then using Lemma 4 with sufficiently large bandwidth causes $20\log_{10}\mathbf{S}^{inp}_{obs}(j\omega_1) = -\infty$ dB and $20\log_{10}\mathbf{T}^{inp}_{obs}(j\omega_1) = 0$ dB. Thus, we get

$$\begin{aligned} \bar{d}(t) &= 10^{\left(20\log_{10}\mathbf{T}^{inp}_{obs}(j\omega_1)/20\right)}\beta_1\sin(\omega_1 t + \gamma_1) \\ &= \beta_1\sin(\omega_1 t + \gamma_1) = d(t) \end{aligned}$$

which completes the proof. □

Remark 4. Corollary 2 implies that enlarging the bandwidth of the controller provides perfect rejection of the sinusoidal disturbances. However, the existence of measurement noise as a practical constraint limits the arbitrary bandwidth enlarging. To decide the bandwidth of the observer under noisy measurements, Lemmas 2–4, Corollaries 1–2 and Fig. 4 should be tackled together.

4.2. Main controller **K**

The goal of the control system **K** of the main loop is to satisfy the internal stability when only the residual disturbance (i.e, $d_{ed} - \bar{d}_{ed}$) is injected into the main loop. For simplicity, we assume that there is no uncertainty on the plant. Then, the procedures given by [25,34] are valid without uncertainties in our numerical simulations.

Remark 5. Note that the goal of the **K** is to assure the internal stability under residual disturbance. The worst-case consideration of the disturbance model directly affects the number of integrators used in augmentation. However, the augmentation procedure is employed just for the virtual-loop. Although less knowledge about the disturbance model increases the conservativeness, employing the augmentation procedure just for the virtual loop, which is an active loop if and only if $d_{ed} \neq 0$, reduces the conservatism.

5. Illustrative examples

In this section, two MIMO examples are presented as simulations. In the first one, 2×2 square MIMO case is investigated. This 2×2 example covers the Section 4.1 and includes a comparison of the proposed method and state-of-art. In the second example, the proposed method is investigated entirely (i.e. this example deals with a range of notions from matching conditions to the whole control system including **K** and $\mathbf{K}_{obs}$) for a 2×3 non-square system.

5.1. Square MIMO system: A comparative study

In this subsection, to have a fair comparison, the virtual loop of Fig. 1 that is shown in Fig. 5(a) is employed merely to focus on the result of Section 4.1. Thus, we only discuss the performance of control system $\mathbf{K}_{obs}$ with respect to the state-of-art methods against polynomial ordered disturbances, sinusoidal disturbances and modeling error. All simulations are carried out through Matlab/Simulink environment using ODE 45 solver.

MIMO four-steering wheel vehicle is taken as a benchmark system. It is a square system with 2-inputs which are steering angles of front and rear tires as $u(t) = [\delta_f\ \delta_r]^T$ and 2-outputs which are side-slip angle and yaw rate as $y(t) = [\beta\ r]^T$. The interested reader should refer to [36] for a detailed discussion of the modeling phase, here, the vehicle model is taken directly from there and is given as

$$\mathbf{A} = \begin{bmatrix} -3.41 & -0.9045 \\ 46.5451 & 3.173 \end{bmatrix}, \mathbf{B} = \begin{bmatrix} 1000 & 2069 \\ 18.046 & -37.3367 \end{bmatrix}, \quad \mathbf{C} = \begin{bmatrix} 1 & 0 \\ 0 & 1 \end{bmatrix} \tag{54}$$

For comparison we used the polynomial differential operator based internal model principle discussed in [23] and we are able to reproduce their results exactly. We then implemented the proposed method on the same complex benchmark and compared the results. The schematic of the IMP controller is shown by Fig. 5(b).

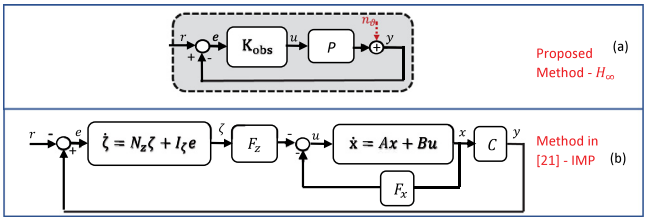

Fig. 5. Compared methods: (a) proposed method - $\mathcal{H}_\infty$, (b) IMP via polynomial differential operator.

Table 1
Test scenarios.

Scenarios	$r(t) = [r_\beta(t)\ r_r(t)]^T$	Uncertainty
I	$r_\beta(t) = 3t^2 + 6t + 4$ $r_r(t) = 3t^2 + 6t + 4$	$\mathbf{P} = \mathbf{P} \times 1$ (No uncertainty)
II	$r_\beta(t) = 3t^2 + 6t + 4 + 1.5\sin(9.42t)$ $r_r(t) = 3t^2 + 6t + 4 + 1.5\sin(9.42t)$	$\mathbf{P} = \mathbf{P} \times 1$ (No uncertainty)
III	$r_\beta(t) = 3t^2 + 6t + 4 + 1.5\sin(9.42t)$ $r_r(t) = 3t^2 + 6t + 4 + 1.5\sin(9.42t)$	$\mathbf{P} = \mathbf{P} \times 0.35$

In this comparison, both methods are tested by three different scenarios and evaluated through two meaningful metrics. These scenarios are given with Table 1 . Note that, the reference signal $r(t)$ is applied to both systems exactly. Moreover, multiplying $\mathbf{B}\times 0.35$ in (54) yields the uncertain systems for the third scenario. On the other hand, to measure the performance of the closed-loop systems, two different metrics on the error of the feedback loop are used. Those are $e(t) = [e_\beta(t)\ e_r(t)]^T = [r_\beta(t) - y_\beta(t)\ r_r(t) - y_r(t)]^T = r(t) - y(t)$ and $\|e(t)\|_2 = \sqrt{e_\beta(t)^2 + e_r(t)^2}$.

5.1.1. Design of $\mathbf{K}_{obs}$ for $\mathcal{H}_\infty$

From this point on the proposed design is carried out by following the procedure in Section 4.1. First, Proposition 1 is satisfied by problem's nature since the polynomial ordered reference signal $r(t)$ is directly chosen as in Table 1 ($y_d(t)$ is represented as $r(t)$). To ensure $e \equiv 0$, we start with 3-fold integral augmentation to get $\mathbf{P}_{aug}$ in (22) as

$$\mathbf{P}_{aug} := \mathbf{P}\mathbf{I}_a = \mathbf{P}\,\mathrm{diag}\left[(1/s^3)\ (1/s^3)\right] \tag{55}$$

Then, noting Assumption 2, to attack (55) with standard tools of $\mathcal{H}_\infty$, we need to employ bilinear transformation with $0 > (-0.05 = \alpha_1) > (-1000 = \alpha_2)$. The resulting system is given by $\mathbf{P}^\star_{aug}$ whose LFT schematic is shown by Fig. 3. Then aim is to design a control system for $\mathbf{P}^\star_{aug}$ via $\mathcal{H}_\infty$ with the following weights

$$\mathbf{W}_{P,obs} = \mathrm{diag}\left[\frac{0.5(s+24.32)^3}{(s+0.8959)^3}\ \frac{0.5(s+24.32)^3}{(s+0.8959)^3}\right] \tag{56}$$

$$\mathbf{W}_{U,obs} = \mathrm{diag}\left[\frac{5000(s+59.61)^2}{(s+1.333\times10^4)^2}\ \frac{5000(s+59.61)^2}{(s+1.333\times10^4)^2}\right]. \tag{57}$$

Having a steeper slope on sensitivity function subjected to $\mathbf{W}_p$ yields the convergent error (to zero) if the growth rate of the exogenous signals have smaller slope than the sensitivity function. Therefore, following (33) provides a bound on the transient dynamics of the closed-loop system if the preceding synthesis is achieved. Moreover, following the schematic guideline that is given in Fig. 4 provides the noise reduction systematically. The graphical representations of (56) is given by Fig. 6(b) As a result, we get (36) as $\|\bar{\mathbf{T}}_{obs}\|_\infty \approx 1.48$ which confirms Lemma 1 and Theorem 2 since we can get a stabilizing controller that satisfies internal stability over (26).

To get the control system given $\mathbf{K}_{obs}$ by Fig. 5(a), first, apply inverse bilinear transformation to obtain $\tilde{\mathbf{K}}_{obs}$ and then virtually

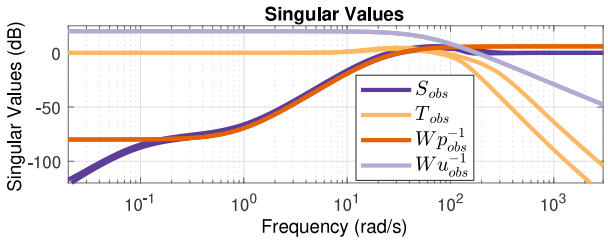

Fig. 6. Sensitivity/Complementary Sensitivity Functions and the weights of the virtual loop.

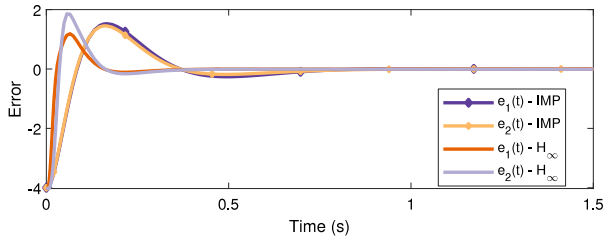

Fig. 7. Results of Scenario I.

augmented integrators should be carried to the controller by re-calling (51). The resulting $\mathbf{K}_{obs}$ is 14th-order.

5.1.2. Design of IMP

The design of the IMP based control is taken from [23] since it is one of the most recent/key studies using IMP for MIMO systems. The parameters that are used in Fig. 5(b) are

$$\mathbf{F}_x = \begin{bmatrix} 1.2630 & 1.5923 \\ -0.5862 & 0.7711 \end{bmatrix}$$

$$\mathbf{F}_z = \begin{bmatrix} -100.7003 & -23.1968 & -1.5543 & 899.5088 & 271.1928 & 30.4197 \\ 66.9356 & 15.7626 & 1.2687 & -437.1666 & -131.6198 & -14.7434 \end{bmatrix}$$

$$\dot{\zeta} = \begin{bmatrix} 0 & 1 & 0 & 0 & 0 & 0 \\ 0 & 0 & 1 & 0 & 0 & 0 \\ 0 & 0 & 0 & 0 & 0 & 0 \\ 0 & 0 & 0 & 0 & 1 & 0 \\ 0 & 0 & 0 & 0 & 0 & 1 \\ 0 & 0 & 0 & 0 & 0 & 0 \end{bmatrix} \zeta + \begin{bmatrix} 0 & 0 \\ 0 & 0 \\ 1 & 0 \\ 0 & 0 \\ 0 & 0 \\ 0 & 1 \end{bmatrix} e$$

5.1.3. Results

The design of the $\mathbf{K}_{obs}$ allowed us to successfully achieve the sensitivity and complementary sensitivity functions as in Fig. 6. The IMP design is resulted in stable closed-loop poles whose places are $\{-10, -11, -12, \ldots, -17\}$.

For the scenario I, both control systems behave similar in terms of the measure metrics. This similarity is shown by Fig. 7. IMP and $\mathcal{H}_\infty$ achieve the tracking of the polynomial-ordered references with zero steady state error, thus, Lemma 3 is validated. Then for the scenario II, the complexity of the problem is increased by adding a sinusoidal extra reference signal in addition to the polynomial one as it described in Table 1. Based on the main design principle and the disadvantages of IMP based control that are mentioned in the Introduction, the performance of the IMP is degraded with respect to $\mathcal{H}_\infty$ as it seen in Fig. 8. This figure also validates the results in Corollary 2 directly. Although it is said that the virtual-loop does not have any uncertainty by its nature since we choose the plant (nominal plant) of the loop virtually, still it is useful to compare the control systems under uncertainty to have a full comparison that covers all aspects. However, with scenario III, IMP and $\mathcal{H}_\infty$ can be distinguished from each other in

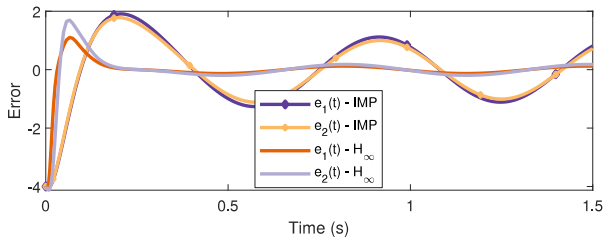

Fig. 8. Results of Scenario II.

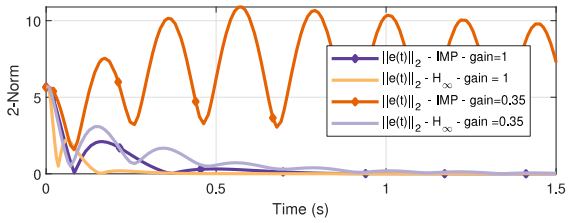

Fig. 9. Results of Scenario III.

terms of tracking performance significantly as it can be seen in Fig. 9.

On the other hand, in order to validate the designed control system under the measurement noise, we have added a new type reference input while preserving all the design operations above. Since the robustness against measurement noise is at the center of interest for this paper, only the proposed method is tested for the noisy case. Here the reference input vector for $t \geq 0$ is selected as unit step signal $r(t) = [1 \ \ -1]^T$ and n_ϑ is selected as band-limited white noise, whose parameters are 3×10^{-6} for the noise power 5×10^{-5} for the sample time. The closed-loop system was also tested for noise free case to represent the noise sensitivity in a comparative manner.

In Fig. 10, controlled system's outputs, control inputs and the band-limited white noise are given as a function of time. This test is repeated two times to get "under noise" condition and "noise free" conditions respectively. Although the control system $\mathbf{K}_{obs}$ includes 3-fold pure integrators on the imaginary-axis, noisy error, which is inevitable, yields a bounded control input signal as anticipated. For the control input, noise free case along with the case under measurement noise are given in Fig. 10. The simulations have shown that results are in good compliance with the theoretical analysis given in Section 4.1 since there is no significant amplifications on the error signal as well as the output response exceeding the bounds of the measurement noise.

5.2. Non-square MIMO example

In this section, as a numerical example, a 2×3 MIMO system is studied to show the effectiveness of the proposed approach.

Consider the following system with the unmatched disturbance as

$$\dot{x}_0(t) = \begin{bmatrix} -9.7 & 3 & 2 \\ 1.4 & -18 & 0.6 \\ 5.1 & 2.2 & -8 \end{bmatrix} x_0(t) + \begin{bmatrix} 0 & 2.2 & 2 \\ 0 & 0.4 & 0 \\ 0.5 & 8.3 & 0 \end{bmatrix} \times u(t) + \begin{bmatrix} 1 & 0 & 0 & 2 \\ 1 & 1 & 1 & 2 \\ 0 & 0 & 1 & 0.4 \end{bmatrix} d(t)$$

$$y_0(t) = \begin{bmatrix} 0.5 & 2 & -1.01 \\ -0.2 & -0.8 & 0.43 \end{bmatrix} x_0(t)$$

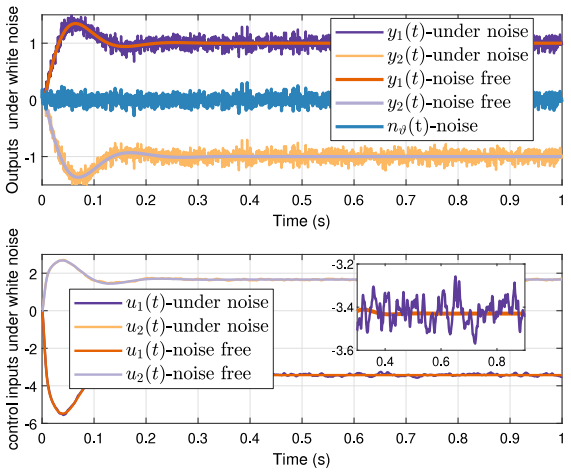

Fig. 10. Control inputs, system outputs and noise signal.

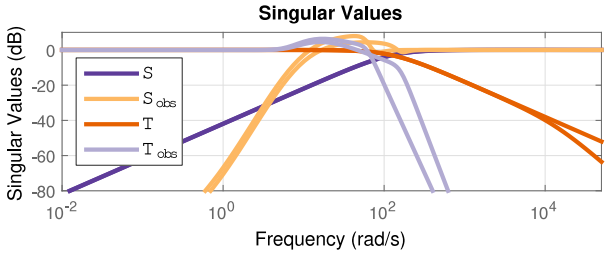

Fig. 11. Sensitivity/complementary sensitivity functions.

where initial conditions are zero, $d(t) = [t^3 \ t^3 \ t^3 \ t^3]^T \notin L_1 \cap L_\infty$. Since $d(t)$ is of polynomial order, $\mathbf{I}_a = \text{diag}[\frac{100}{s^4} \ \frac{100}{s^4}]$. The performance weights used in the synthesis of $\mathbf{K}$ and $\mathbf{K}_{obs}$ are given as follows respectively.

$$\mathbf{W}_P = \text{diag}[\frac{0.5(s+125.7)}{(s+0.0006)} \ \frac{0.5(s+125.7)}{(s+0.0006)}],$$

$$\mathbf{W}_{P,obs} = \text{diag}[\frac{0.5(s+12.24)^4}{(s+0.5789)^4} \ \frac{0.5(s+23.78)^4}{(s+0.63)^4}]$$

$$\mathbf{W}_U = \mathbf{W}_{U,obs} = \text{diag}[0.00001 \ 0.00001 \ 0.00001]$$

The solutions of the corresponding $\mathcal{H}_\infty$-Synthesis are given in Fig. 11 in terms of sensitivity/complementary sensitivity functions. The resulting $\mathbf{K}_{obs}$ is 27th-order.Following the procedure described in Section 3.1 yields d_{ed} and $\bar{d}_{ed}$ that are shown in Fig. 12. For identical $u(t)$ for both systems, the difference between (1)–(2) (i.e., $y_0(t) - y(t)$) is depicted in Fig. 13 which shows that conditions of Definition 1 are satisfied under unbounded polynomial disturbances. Using $d(t)$ and $d_{ed}(t)$ in Fig. 12, in Fig. 14, we can observe that $\lim_{t\to\infty}(y(t) - \bar{y}(t)) = 0$ and $\|y(t) - \bar{y}(t)\|_2 \approx 0.001$ such that Definition 2 is satisfied.

The reason behind the difference between the exact-equivalent disturbances and the estimator output given by Fig. 12, there is no unique solution as it can be seen in Section 3.1.1. In addition, the errors in Fig. 13 are very small and are mostly due to numerical computations.

6. Conclusions

In this paper, necessary and sufficient conditions for the transformation between matched and unmatched disturbances have been investigated and a new and more relaxed definition for EID (namely S-EID) has been given. Analytical solutions and numerical examples have shown that there exist matched equivalents of

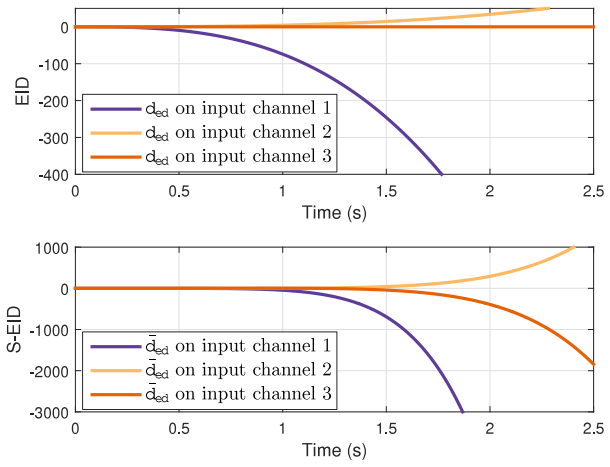

Fig. 12. $d_{ed}(t)$ and $\bar{d}_{ed}(t)$ for the polynomial $d(t)$.

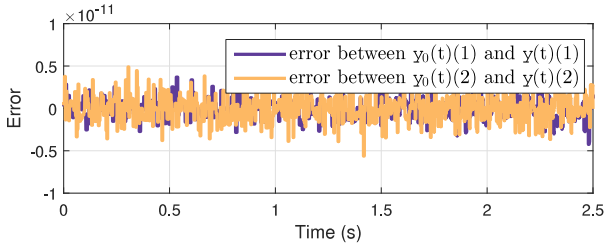

Fig. 13. The error between $y_0(t) - y(t)$ (i.e. for $\mathbf{B}_d d(t)$ and $\mathbf{B}d_{ed}(t)$ cases).

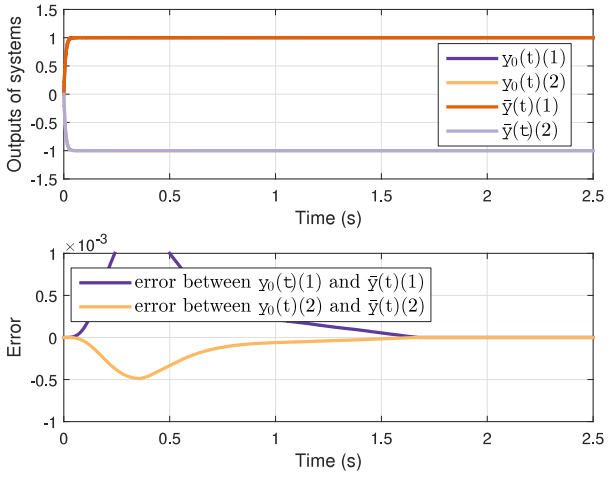

Fig. 14. Overall architecture's performance with active disturbance rejection under polynomial disturbances and the one with equivalent case.

the unmatched disturbances for a wide range of disturbance and system types. Therefore, focusing on the rejection and estimation of the EID would be sufficient for many cases. Theoretical results have shown that the existence of the EID/S-EID depends on both the system and the disturbance characteristics. In addition, it has been observed that under polynomial references/disturbances, it is possible to design a control system such that the effects of those exogenous signals can be minimized with the help of multiple integral augmentation and standard $\mathcal{H}_\infty$-synthesis. It has been also worth mentioning that considering unit step, impulse, and ramp type, as well as harmonic disturbance, is sufficient for most real-world problems. However, as noted in the introduction section, the number of applications affected by polynomial-type disturbances is spreading. Thus, having the mathematical foundations of dealing with polynomial-type disturbances enables solving new types of robust control problems.

The proposed method includes several theoretical and practical challenges. As the number of integrators increases, the difficulties of finding a stabilizing controller under high-performance conditions against polynomial type disturbances/references and low noise sensitivity of the feedback loop increases. In the practical sense, augmenting multiple integrators increases the order of the resulting control system additionally even though the order of the synthesized controllers of $\mathcal{H}_\infty$ is high in its nature.

Future research directions include expansion of the theory to unmatched uncertainties and nonlinear systems.

Declaration of competing interest

The authors declare that they have no known competing financial interests or personal relationships that could have appeared to influence the work reported in this paper.

References

[1] Khalil HK, Grizzle JW. Nonlinear systems, Vol. 3. Upper Saddle River, NJ: Prentice hall; 2002.
[2] Yang J, Chen W-H, Li S. Non-linear disturbance observer-based robust control for systems with mismatched disturbances/uncertainties. IET Control Theory Appl 2011;5(18):2053–62.
[3] Han J, Liu X, Gao X, Wei X. Intermediate observer-based robust distributed fault estimation for nonlinear multiagent systems with directed graphs. IEEE Trans Ind Inf 2019;16(12):7426–36.
[4] Liu X, Gao X, Han J. Distributed fault estimation for a class of nonlinear multiagent systems. IEEE Trans Syst Man Cybern: Syst 2018;50(9):3382–90.
[5] Qiao J, Li Z, Xu J, Yu X. Composite nonsingular terminal sliding mode attitude controller for spacecraft with actuator dynamics under matched and mismatched disturbances. IEEE Trans Ind Inf 2019;16(2):1153–62.
[6] Guo B, Chen Y. Adaptive fault tolerant control for time-varying delay system with actuator fault and mismatched disturbance. ISA Trans 2019;89:122–30.
[7] Misra G, Bai X. Robust disturbance observer-based control for relative attitude tracking using sum-of-squares programming. J Guid Control Dyn 2020;43(4):806–13.
[8] She J-H, Kobayashi H, Ohyama Y, Xin X. Disturbance estimation and rejection-An equivalent input disturbance estimator approach. In: 2004 43rd IEEE conference on decision and control (CDC)(IEEE Cat. No. 04CH37601), Vol. 2. IEEE; 2004, p. 1736–41.
[9] She J-H, Fang M, Ohyama Y, Hashimoto H, Wu M. Improving disturbance-rejection performance based on an equivalent-input-disturbance approach. IEEE Trans Ind Electron 2008;55(1):380–9.
[10] Li M, She J, Zhang C-K, Liu Z-T, Wu M, Ohyama Y. Active disturbance rejection for time-varying state-delay systems based on equivalent-input-disturbance approach. ISA Trans 2021;108:69–77.
[11] Kürkçü B, Kasnakoğlu C, Efe MO. Disturbance/uncertainty estimator based integral sliding-mode control. IEEE Trans Automat Control 2018;63(11):3940–7.
[12] Tian J, Zhang S, Zhang Y, Li T. Active disturbance rejection control based robust output feedback autopilot design for airbreathing hypersonic vehicles. ISA Trans 2018;74:45–59.
[13] Du Y, Cao W, She J, Wu M, Fang M, Kawata S. Disturbance rejection and control system design using improved equivalent input disturbance approach. IEEE Trans Ind Electron 2019;67(4):3013–23.
[14] Hunt L, Meyer G, Su R. Noncausal inverses for linear systems. IEEE Trans Automat Control 1996;41(4):608–11.
[15] Xargay E, Hovakimyan N, Cao C. L 1 adaptive controller for multi-input multi-output systems in the presence of nonlinear unmatched uncertainties. In: Proceedings of the 2010 American control conference. IEEE; 2010, p. 874–9.
[16] Guo K, Jia J, Yu X, Guo L, Xie L. Multiple observers based anti-disturbance control for a quadrotor UAV against payload and wind disturbances. Control Eng Pract 2020;102:104560.
[17] Do TD, Nguyen HT. A generalized observer for estimating fast–varying disturbances. IEEE Access 2018;6:28054–63.

[18] Kim K-S, Rew K-H, Kim S. Disturbance observer for estimating higher order disturbances in time series expansion. IEEE Trans Automat Control 2010;55(8):1905–11.
[19] Yan Y, Zhang C, Liu C, Yang J, Li S. Disturbance rejection for nonlinear uncertain systems with output measurement errors: Application to a helicopter model. IEEE Trans Ind Inf 2019;16(5):3133–44.
[20] Cordero R, Estrabis T, Gentil G, Batista E, Andrea C. Development of a generalized predictive control system for polynomial reference tracking. IEEE Trans Circuits Syst II 2021.
[21] Francis BA, Wonham WM. The internal model principle of control theory. Automatica 1976;12(5):457–65.
[22] Serrani A, Isidori A, Marconi L. Semi-global nonlinear output regulation with adaptive internal model. IEEE Trans Automat Control 2001;46(8):1178–94.
[23] Kim SB, Kim DH, Pratama PS, Kim JW, Kim HK, Oh SJ, Jung YS. MIMO robust servo controller design based on internal model principle using polynomial differential operator. In: AETA 2015: Recent advances in electrical engineering and related sciences. Springer; 2016, p. 469–84.
[24] Chiang R, Safonov M. H-infinity synthesis using a bilinear pole shifting transform. J Guid Control Dyn 1992;15(5):1111–7.
[25] Kürkçü B, Kasnakoğlu C, Efe MO. Disturbance/uncertainty estimator based robust control of nonminimum phase systems. IEEE/ASME Trans Mechatronics 2018;23(4):1941–51.
[26] Zhou K, Doyle JC. Essentials of robust control, Vol. 104. Upper Saddle River, NJ: Prentice hall; 1998.
[27] Zhang F. The Schur complement and its applications, Vol. 4. Springer Science & Business Media; 2006.
[28] Åström KJ, Murray RM. Feedback systems: an introduction for scientists and engineers. Princeton, NJ: Princeton university press; 2008.
[29] Lundström P, Skogestad S, Wang Z-Q. Performance weight selection for H-infinity and μ-control methods. Trans Inst Meas Control 1991;13(5):241–52.
[30] Chen J. Logarithmic integrals, interpolation bounds, and performance limitations in MIMO feedback systems. IEEE Trans Automat Control 2000;45(6):1098–115.
[31] Looze DP, Freudenberg JS. Limitations of feedback properties imposed by open-loop right half plane poles. IEEE Trans Automat Control 1991;36(6):736–9.
[32] Paige C, Van Loan C. A schur decomposition for Hamiltonian matrices. Linear Algebra Appl 1981;41:11–32.
[33] Glover K, Doyle JC. State-space formulae for all stabilizing controllers that satisfy an H-norm bound and relations to relations to risk sensitivity. Systems Control Lett 1988;11(3):167–72.
[34] Kürkçü B, Kasnakoğlu C. Robust autopilot design based on a disturbance/uncertainty/coupling estimator. IEEE Trans Control Syst Technol 2019;27(6):2622–9.
[35] Coral-Enriquez H, Pulido-Guerrero S, Cortés-Romero J. Robust disturbance rejection based control with extended-state resonant observer for sway reduction in uncertain tower-cranes. Int J Autom Comput 2019;16(6):812–27.
[36] Lv H, Liu S. Closed-loop handling stability of 4WS vehicle with yaw rate control. Stroj Vestnik-J Mech Eng 2013;59(10):595–603.